Electronic Supplementary Information (ESI) available for:

Synthesis, molecular structure, computational study and *in vitro* anticancer activity of dinuclear thiolato-bridged pentamethylcyclopentadienyl Rh(III) and Ir(III) complexes

Gajendra Gupta,[a] Amine Garci,[a] Benjamin S. Murray,[b] Paul J. Dyson,[b] Gabin Fabre,[c,d] Patrick Trouillas,[c,d,e] Federico Giannini,[a,f] Julien Furrer,[f] Georg Süss-Fink[a] and Bruno Therrien*[a]

[a] *Institute of Chemistry, University of Neuchatel, Ave de Bellevaux 51, CH-2000 Neuchatel, Switzerland: Fax:(+41) 32 718 2511; Tel: +41 32 718 2499; E-mail:bruno.therrien@unine.ch*
[b] *Institut des Sciences et Ingénierie Chimiques, Ecole Polytechnique Fédérale de Lausanne (EPFL), CH-1015 Lausanne, Switzerland.*
[c] *LCSN-EA1069, Faculté de Pharmacie, Université de Limoges, 2 rue du Dr. Marcland, 87025 Limoges, France.*
[d] *Department of Physical Chemistry, University of Olomouc, tř. 17. listopadu 12, 771 46 Olomouc, Czech Republic.*
[e] *Laboratoire de Chimie des Matériaux Nouveaux, Université de Mons, Place du Parc 20, 7000 Mons, Belgium.*
[f] *Department für Chemie und Biochemie, Universität Bern, CH-3012 Bern, Switzerland.*

*Corresponding author. E-mail: bruno.therrien@unine.ch FAX +41-32-7182511

Table S1. Selected bond lengths and angles for **1**, **2** and [**6**]Cl · HCl.

	1	**2**	[**6**]Cl · HCl
Interatomic distances (Å)			
M1-S1	2.3725(17)	2.3903(17)	2.3793(18)
M1-S2	2.3681(17)	2.3676(13)	2.3822(17)
Ir1-S3	-	-	2.3945(15)
M2-S1	2.3711(18)	2.3807(13)	2.3866(18)
M2-S2	2.3688(15)	2.3682(15)	2.3823(17)
Ir2-S3	-	-	2.4007(16)
Rh1-Cl1	2.3802(17)	2.3869(11)	-
Rh2-Cl2	2.3884(16)	2.3778(10)	-
Angles (°)			
M1-S1-M2	100.10(7)	99.22(6)	88.89(6)
M1-S2-M2	100.29(6)	100.22(6)	88.92(5)
Ir1-S3-Ir2	-	-	88.20(5)
Cl1-Rh1-S1	94.73(6)	95.25(5)	-
Cl1-Rh1-S2	95.09(6)	95.01(4)	-
Cl2-Rh2-S1	95.63(6)	92.93(4)	-
Cl2-Rh2-S2	94.11(6)	95.12(5)	-

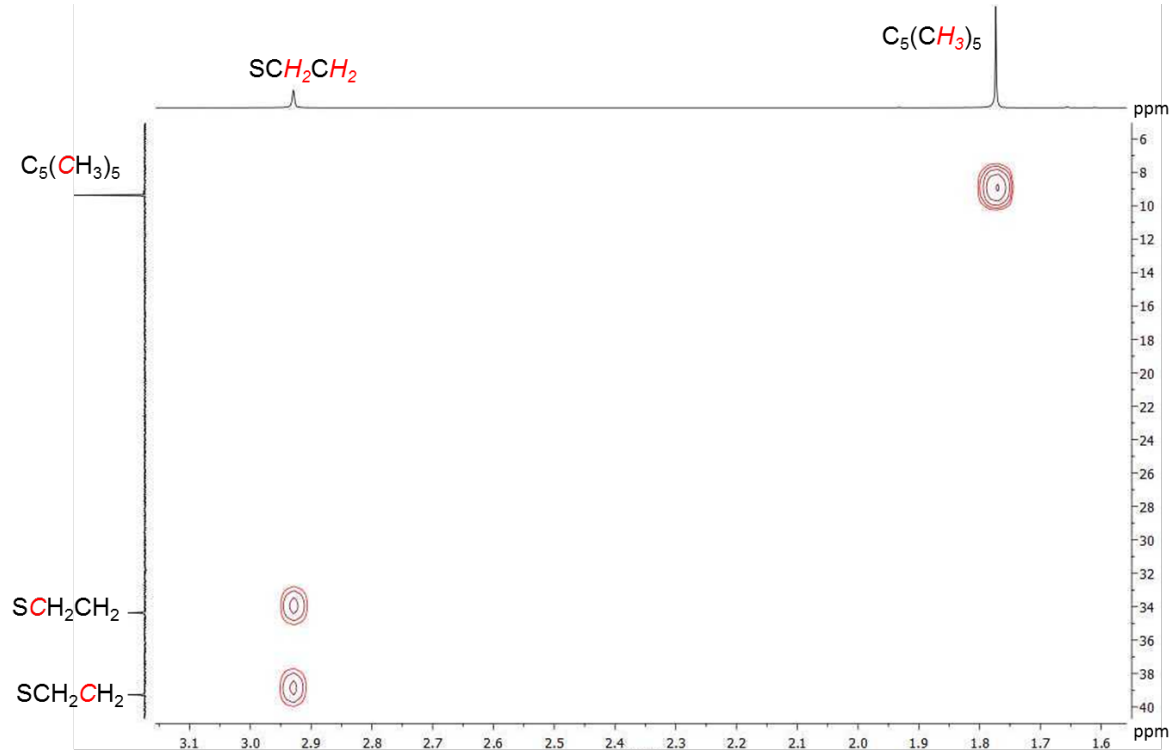

Figure S1. 2D HSQC proton-carbon COSY experiment of [**6**]Cl in CD_2Cl_2.

Experimental part

General

The starting materials $[(C_5Me_5)_2Rh_2(\mu\text{-}Cl)_2Cl_2]$ and $[(C_5Me_5)_2Ir_2(\mu\text{-}Cl)_2Cl_2]$ were prepared according to published methods.[1] All other reagents were commercially available and used without further purification. The ^1H and $^{13}C\{^1H\}$ NMR spectra were recorded with a Bruker Avance II 500 or a Bruker Avance II 400 MHz spectrometer using the residual protonated solvent. Infrared spectra were recorded as KBr pellets with a Perkin-Elmer FTIR 1720 X spectrometer. Electrospray mass spectra were obtained in positive- or negative ion mode with an LCQ Finnigan mass spectrometer. Microanalyzes were carried out by the Mikroelementaranalytisches Laboratorium, ETH Zürich (Switzerland). UV/Vis absorption spectra were recorded with an Uvikon 930 spectrophotometer (10^{-5} M in CH_2Cl_2).

Synthesis of the neutral complexes 1 and 2

The dinuclear complex $[(C_5Me_5)_2Rh_2(\mu\text{-}Cl)_2Cl_2]$ (100 mg, 0.16 mmol) is first dissolved in technical-grade ethanol (10-12 mL). When the compound is completely dissolved, the solution is cooled to 0 ºC. After addition of the corresponding thiol (0.34 mmol; $PhCH_2SH$ (**1**): 38 µL, $PhCH_2CH_2SH$ (**2**): 43.4 µL), the solution is stirred at 0 ºC for 2-3 hours. The color of the solution turns dark red. Then the volume is reduced to about 2 mL and diethyl ether is slowly added to initiate the precipitation. After being kept in the freezer overnight, the orange red crystalline product is centrifuged, filtered, washed with diethyl ether, and dried under vacuum.

Complex 1. Yield: 85 mg (66%). ESI MS (MeOH, CH_2Cl_2): *m/z* = 758.0 $[M\text{-}Cl]^+$. ^1H NMR (400 MHz, CD_2Cl_2): δ = 7.28 (m, 10H, $CH_2C_6\mathit{H}_5$), 3.70 (s, 4H, $SC\mathit{H}_2$), 1.41 (s, 30H, C_5Me_5) ppm. $^{13}C\{^1H\}$ NMR (100 MHz, CH_2Cl_2): δ = 8.59, 34.84, 96.70, 126.32, 128.20, 131.08 ppm. UV/Vis (1.0×10^{-5} M, CH_2Cl_2, 298 K): λ_{max} nm (ε cm^{-1}) = 214 (38954), 305 (25920), 395 (7988). IR (KBr pellets, cm^{-1}): *ν* = 3437 (w, CH_{aryl}) and 702 (s, CH_2-S). Anal. Calcd for $C_{34}H_{44}Cl_2Rh_2S_2 \cdot 2\ H_2O$: C, 49.22; H, 5.83; Found C, 48.87; H, 5.59%.

Complex 2. Yield: 80 mg (60%). ESI MS (MeOH, CH_2Cl_2): *m/z* = 786.2 $[M\text{-}Cl]^+$. ^1H NMR (400 MHz, CD_2Cl_2): δ = 7.28 (m, 10H, $CH_2CH_2C_6\mathit{H}_5$), 2.71 (t, 4H, *J* = 4 Hz, $SC\mathit{H}_2C\mathit{H}_2$), 2.63 (t, 4H, *J* = 4 Hz, $SC\mathit{H}_2C\mathit{H}_2$), 1.64 (s, 30H, C_5Me_5) ppm. $^{13}C\{^1H\}$ NMR (100 MHz, CH_2Cl_2): δ = 8.98, 32.04, 38.00, 96.70, 126.01, 128.46, 129.10 ppm. UV/Vis (1.0×10^{-5} M,

CH_2Cl_2, 298 K): λ_{max} nm (ε cm^{-1}) = 229 (50094), 306 (39929), 387 (15077). IR (KBr pellets, cm^{-1}): ν = 3436 (w, CH_{aryl}) and 717 (s, CH_2-S). Anal. Calcd for $C_{36}H_{48}Cl_2Rh_2S_2 \cdot H_2O$: C, 51.50; H, 6.00; Found C, 51.02; H 5.68%.

Synthesis of [3]Cl – [8]Cl

The dinuclear complex $[(C_5Me_5)_2M_2(\mu\text{-}Cl)_2Cl_2]$ (M = Rh, 100 mg, 0.16 mmol; M = Ir, 100 mg, 0.13 mmol) is refluxed in technical-grade ethanol (25 mL). When the compound is completely dissolved, an ethanolic solution (5 mL) of the corresponding thiol (M = Rh, 0.48 mmol; $PhCH_2SH$, 57 µL (**3**); $PhCH_2CH_2SH$, 65 µL (**5**); *p*-^{t}Bu-C_6H_4-CH_2SH, 90.6 µL (**7**): M = Ir, 0.39 mmol; $PhCH_2SH$, 44.2 µL (**4**); $PhCH_2CH_2SH$, 50.5 µL (**6**); *p*-^{t}Bu-C_6H_4-CH_2SH, 70.3 µL (**8**)) is added dropwise to the hot solution. The resulting solution is refluxed for 3 hours, the color of the solution changed to red for the rhodium derivatives and to yellow for the iridium derivatives. The mixture is cooled down and the solvent removed under reduced pressure. The reddish or yellowish oil is washed several times with diethyl ether and hexane to obtain a fine powder. The powder is dissolved in dichloromethane, precipitated one more time by adding diethyl ether, and after being filtered, the compound is dried under vacuum.

Compound [3]Cl. Yield: 92 mg (65%). ESI MS (MeOH, CH_2Cl_2): *m/z* = 846.0 $[M\text{-}Cl]^+$. ^1H NMR (400 MHz, CD_2Cl_2): δ = 7.46 (m, 15H, $CH_2C_6H_5$), 3.80 (s, 6H, SCH_2), 1.55 (s, 30H, C_5Me_5) ppm. $^{13}C\{^1H\}$ NMR (100 MHz, CH_2Cl_2): δ = 9.69, 37.06, 98.90, 127.92, 129.02, 129.17 ppm. UV/Vis (1.0 x 10^{-5} M, CH_2Cl_2, 298 K): λ_{max} nm (ε cm^{-1}) = 229 (40568), 285 (58324), 381 (13563). IR (KBr pellets, cm^{-1}): ν = 3409 (w, CH_{aryl}) and 703 (s, CH_2-S). Anal. Calcd for $C_{41}H_{51}Rh_2S_3Cl \cdot HCl$: C, 53.66; H, 5.71; Found C, 52.96; H, 5.94%.

Compound [4]Cl. Yield: 104 mg (78%). ESI MS (MeOH, CH_2Cl_2): *m/z* = 1024.3 $[M\text{-}Cl]^+$. ^1H NMR (400 MHz, CD_2Cl_2): δ = 7.46 (m, 15H, $CH_2C_6H_5$), 4.02 (s, 6H, SCH_2), 1.56 (s, 30H, C_5Me_5) ppm. $^{13}C\{^1H\}$ NMR (100 MHz, CH_2Cl_2): δ = 9.51, 36.79, 92.70, 128.11, 129.06, 129.11 ppm. UV/Vis (1.0 x 10^{-5} M, CH_2Cl_2, 298 K): λ_{max} nm (ε cm^{-1}) = 238 (36771), 314 (12172). IR (KBr pellets, cm^{-1}): ν = 3430 (w, CH_{aryl}) and 703 (s, CH_2-S). Anal. Calcd for $C_{41}H_{51}Ir_2S_3Cl \cdot HCl$: C, 44.91; H, 4.78; Found C, 44.69; H, 4.77%.

Compound [5]Cl. Yield: 107 mg (72%). ESI MS (MeOH, CH_2Cl_2): *m/z* = 888.1 $[M\text{-}Cl]^+$. ^1H NMR (400 MHz, CD_2Cl_2): δ = 7.30 (m, 15H, $CH_2CH_2C_6H_5$), 2.97 (t, 6H, *J* = 8 Hz, SCH_2CH_2), 2.70 (t, 6H, *J* = 8 Hz, SCH_2CH_2), 1.71 (s, 30H, C_5Me_5) ppm. $^{13}C\{^1H\}$ NMR (100 MHz, CH_2Cl_2): δ = 9.53, 34.73, 40.36, 98.22, 127.20, 128.96, 129.15 ppm. UV/Vis (1.0

x 10^{-5} M, CH_2Cl_2, 298 K): λ_{max} nm (ε cm^{-1}) = 229 (32900), 283 (69940), 383 (15472). IR (KBr pellets, cm^{-1}): ν = 3419 (w, CH_{aryl}) and 716 (s, CH_2-S). Anal. Calcd for $C_{44}H_{57}Rh_2S_3Cl \cdot HCl$: C, 55.06; H, 6.09; Found C, 55.48; H, 6.16%.

Compound [6]Cl. Yield: 121 mg (87%). ESI MS (MeOH, CH_2Cl_2): *m/z* = 1066.4 $[M\text{-}Cl]^+$. ^1H NMR (400 MHz, CD_2Cl_2): δ = 7.30 (m, 15H, $CH_2CH_2C_6H_5$), 2.94 (s, 12H, SCH_2CH_2), 1.77 (s, 30H, C_5Me_5) ppm. $^{13}C\{^1H\}$ NMR (100 MHz, CH_2Cl_2): δ = 9.36, 34.36, 39.27, 91.91, 127.21, 128.91, 129.18 ppm. UV/Vis (1.0 x 10^{-5} M, CH_2Cl_2, 298 K): λ_{max} nm (ε cm^{-1}) =228 (34569), 314 (13890). IR (KBr pellets, cm^{-1}): ν = 3448 (w, CH_{aryl}) and 759 (s, CH_2-S). Anal. Calcd for $C_{44}H_{57}Ir_2S_3Cl \cdot 2\ HCl$: C, 44.98; H, 5.06; Found C, 45.50; H, 5.34%.

Compound [7]Cl. Yield: 80 mg (47%). ESI MS (MeOH, CH_2Cl_2): *m/z* = 1014.1 $[M\text{-}Cl]^+$. ^1H NMR (400 MHz, CD_2Cl_2): δ = 7.53 (d, *J* = 8 Hz, 6H, $CH_2C_6H_4$-*p*-^{t}Bu), 7.47 (d, *J* = 8 Hz, 6H, $CH_2C_6H_4$-*p*-^{t}Bu), 3.75 (s, 6H, SCH_2), 1.54 (s, 30H, C_5Me_5), 1.37 (s, 27H, $CH_2C_6H_4$-*p*-^{t}*Bu*) ppm. $^{13}C\{^1H\}$ NMR (100 MHz, CH_2Cl_2): δ = 9.64, 31.42, 34.84, 36.71, 98.81, 125.86, 125.88, 137.05 ppm. UV/Vis (1.0 x 10^{-5} M, CH_2Cl_2, 298 K): λ_{max} nm (ε cm^{-1}) = 229 (43687), 286 (44523), 383 (12712). IR (KBr pellets, cm^{-1}): ν = 3400 (w, CH_{aryl}) and 704 (s, CH_2-S). Anal. Calcd for $C_{53}H_{75}Rh_2S_3Cl \cdot HCl$: C, 58.61; H, 7.05; Found C, 58.92; H, 7.06%.

Compound [8]Cl. Yield: 78 mg (51%). ESI MS (MeOH, CH_2Cl_2): *m/z* = 1192.5 $[M\text{-}Cl]^+$. ^1H NMR (400 MHz, CD_2Cl_2): δ = 7.51 (d, *J* = 8 Hz, 6H, $CH_2C_6H_4$-*p*-^{t}Bu), 7.46 (d, *J* = 8 Hz, 6H, $CH_2C_6H_4$-*p*-^{t}Bu), 3.96 (s, 6H, SCH_2), 1.54 (s, 30H, C_5Me_5), 1.36 (s, 27H, $CH_2C_6H_4$-*p*-^{t}*Bu*) ppm. $^{13}C\{^1H\}$ NMR (100 MHz, CH_2Cl_2): δ = 9.44, 31.40, 34.87, 36.41, 92.62, 125.89, 128.83, 136.43 ppm. UV/Vis (1.0 x 10^{-5} M, CH_2Cl_2, 298 K): λ_{max} nm (ε cm^{-1}) = 238 (44361), 315 (10606). IR (KBr pellets, cm^{-1}): ν = 3423 (w, CH_{aryl}) and 703 (s, CH_2-S). Anal. Calcd for $C_{53}H_{75}Ir_2S_3Cl \cdot HCl$: C, 50.33; H, 6.06; Found C, 50.75; H, 6.03%.

Single-crystal X-ray structure analyses

Crystals of compounds **1**, **2** and [**6**]Cl · HCl were mounted on a Stoe Image Plate Diffraction system equipped with a ϕ circle goniometer, using Mo-Kα graphite monochromatic radiation (λ = 0.71073 Å) with ϕ range 0-200°. The structures were solved by direct methods using the program SHELXS-97, while the refinement and all further calculations were carried out using SHELXL-97.[2] The H-atoms were included in calculated positions and treated as riding atoms using the SHELXL default parameters. The non-H atoms were refined anisotropically, using weighted full-matrix least-square on F^2. The completeness of all data sets is low and the

pentamethylcyclopentadienyl rings are often disordered over several positions. However, the quality of the data remains satisfying, while modelling of the pentamethylcyclopentadienyl rings over two or more positions did not significantly improve the structures. Based on the reaction conditions, the localized electron densities observed with cation **6** in [**6**]Cl have been assigned to Cl and HCl respectively. However some ambiguity remains about these assignments. Crystallographic details for **1**, **2** and [**6**]Cl · HCl are summarised in Table S2. Figures 3 and 4 were drawn with ORTEP.[3]

CCDC-939466 **1** and 939467 **2** and 939468 [**6**]Cl · HCl contain the supplementary crystallographic data for this paper. These data can be obtained free of charge at www.ccdc.cam.ac.uk/conts/retrieving.html [or from the Cambridge Crystallographic Data Centre, 12, Union Road, Cambridge CB2 1EZ, UK; fax: (internat.) +44-1223/336-033; E-mail: deposit@ccdc.cam.ac.uk].

Table S2. Crystallographic and structure refinement parameters for **1**, **2** and [**6**]Cl · HCl.

	1	**2**	[**6**]Cl · HCl
Chemical formula	$C_{34}H_{44}Cl_2Rh_2S_2$	$C_{36}H_{48}Cl_2Rh_2S_2$	$C_{44}H_{57}Cl_2Ir_2S_3$
Formula weight	793.53	821.58	1138.38
Crystal system	Monoclinic	Monoclinic	Triclinic
Space group	*P n* (no. 7)	*C* 2/*c* (no. 15)	*P* -1 (no. 2)
Crystal colour and shape	Orange block	Orange block	Yellow block
Crystal size	0.19 x 0.18 x 0.14	0.19 x 0.15 x 0.13	0.23 x 0.21 x 0.14
a (Å)	8.7743(7)	21.115(4)	11.350(2)
b (Å)	14.8192(13)	17.085(3)	12.320(2)
c (Å)	13.3856(12)	20.881(4)	17.097(3)
α (°)	90	90	88.82(3)
β (°)	91.358(10)	103.72(3)	76.00(3)
γ (°)	90	90	71.04(3)
V (Å^3)	1740.0(3)	7318(2)	2189.5(7)
Z	2	8	2
T (K)	173(2)	173(2)	173(2)
D_c (g·cm^{-3})	1.515	1.491	1.727
μ (mm^{-1})	1.243	1.185	6.366
Scan range (°)	3.04 < θ < 26.09	2.34 < θ < 26.11	2.04 < θ < 26.13
Unique reflections	6136	6414	7921
Observed refls [I>2σ(I)]	4955	3199	5142
R_{int}	0.0321	0.0474	0.0366
Final *R* indices [I>2σ(I)]*	0.0313, wR_2 0.0752	0.0323, wR_2 0.0651	0.0267, wR_2 0.0491
R indices (all data)	0.0455, wR_2 0.0872	0.0873, wR_2 0.0774	0.0551, wR_2 0.0548
Goodness-of-fit	1.000	0.764	0.816
Max, Min Δρ/e (Å^{-3})	0.416, - 0.366	0.648, - 0.616	0.689, - 0.668

* Structures were refined on F_0^2: $wR_2 = [\Sigma[w (F_0^2 - F_c^2)^2] / \Sigma w (F_0^2)^2]^{1/2}$, where $w^{-1} = [\Sigma(F_0^2) + (aP)^2 + bP]$ and $P = [\max(F_0^2, 0) + 2F_c^2]/3$

Computational methodology

The initial structures were obtained from the X-ray crystallography data. These structures were then optimized using DFT (density functional theory) with the B3LYP hybrid functional, well-adapted to evaluate conformational and energetic features of such molecular assemblies. To assess electronic energies, the 6-31+G(d,p) basis set was used for all atoms except the metals, for which the Lanl2DZ pseudo-potential was used. The corrections to enthalpy and Gibbs energy (298 K, 1 atm) were calculated based on the frequency analysis

performed with the 6-31G(d) basis set (based on B3LYP/6-31G(d) geometries). Basis set effects were also evaluated on electronic energy, using the more robust (but computationally too high-costing for frequency analysis) def2-TZVPP basis set for the H, C, S and Cl atoms, and the adapted ecpdef2-TZVPP pseudo potential for the metals; this calculation has improved validation of our methodology, as the difference in electronic energies $\Delta E_{syn\text{-}anti}$ were very similar than those obtained with the Pople-type 6-31+G(d,p) basis set.

As using explicit solvent would be computationally unfeasible regarding the number of degrees of freedom for these organometallic complexes, implicit solvent models were used to tackle solvent effects, namely in our case dichloromethane solvation. IEFPCM (integral equation formalism of the polarizable continuum method) or COSMO (conductor-like screening model) were used with both types of basis sets, respectively. Both solvent models consider the solute embedded in a shape-adapted cavity surrounded by a dielectric continuum characterized by its dielectric constant i.e., $\varepsilon = 8.93$ for dichloromethane. The IEFPCM-B3LYP/6-31+G(d,p)(Lanl2DZ) and COSMO-B3LYP/def2-TZVPP(ecpdef2-TZVPP) calculations were performed with the Gaussian09 and Orca programs, respectively.

Concerning population analysis, the atomic charges were obtained from electrostatic potentials using a grid based method (CHELPG).

Cell culture and inhibition of cell growth

Human A2780 and A2780cisR ovarian carcinoma cells and HEK293 cells were obtained from the European Collection of Cell Cultures (ECACC) (Salisbury, UK). Cells were cultured in either RPMI-1640 with GlutaMAX (A2780, A2780cisR) or DMEM high glucose with GlutaMAX (HEK 293) medium containing 10 % fetal bovine serum (FBS) and penicillin at 37ºC and 5% CO_2. Cytotoxicity was determined using the MTT assay.[4] Cells were seeded in 96 well plates by the addition of cells as a suspension in their respective media containing 10 % FBS (100 µl per well, approximately 5000 cells) and pre-incubated for 24 h.

Stock solutions of the compounds were prepared in DMSO then diluted by addition to the culture medium (RPMI or DMEM for A2780 and A2780cisR or HEK 293, respectively). The stock solutions were then serially diluted to give compound solutions of the desired concentrations. Complex solutions (100 µl) were then added to plate wells (yielding final compound solutions in the range 0 to 5 µM) and the plates incubated for a further 72 h.

Subsequently, MTT (3-(4,5-dimethyl-2-thiazolyl)-2,5-diphenyl-2H-tetrazolium bromide) solution (20 µl, 5 mg/mL in H_2O) was added to each well and the plates incubated for a further 2 h. The culture medium was then aspirated and the violet formazan precipitate produced by mitochondrial dehydrogenases of living cells was dissolved by the addition of DMSO (100 µl) to each well. The absorbance of the resultant solutions at 590 nm, which is directly proportional to the number of surviving cells, was recorded using a multiwall plate reader. The percentage of surviving cells was determined by measurement of the absorbance of wells corresponding to untreated control cells. The reported IC_{50} values are based on the mean values from two independent experiments; each concentration level per experiment was evaluated in triplicate, and those values are reported in Table 4.

Catalytic oxidation of glutathione analyzed by NMR spectroscopy

NMR data were acquired at 37°C using a Bruker Avance II 500-MHz NMR spectrometer equipped with an inverse 1.7 mm dual channel (^{1}H, X) *z*-gradient microprobe head. One-dimensional ^{1}H NMR data were acquired with 128 transients as 65,536 data points over a width of 12 ppm using a classical presaturation to eliminate the water resonance. A relaxation delay of 4 s was applied between the transients. All NMR data were processed using Topspin (version 2.1 or 3.0, Bruker, Switzerland). The ^{1}H δ scale was referenced to the residual water signal at 4.637 ppm (δ H_2O at 37 °C). To evaluate the catalytic performance of the complexes for the oxidation of GSH to GSSG, the complexes (approximately 1.5 mM) were dissolved in a mixture D_2O/DMSO-d_6 (99.5:0.5) and 10 equivalent of GSH was added to the solution. The samples were subsequently analyzed by ^{1}H NMR spectroscopy. For the eight complexes, the ^{1}H NMR spectra were recorded immediately after sample preparation, and then every 30 minutes until almost complete disappearance of the original resonances of GSH. The TOF_{50} values were obtained from each catalytic run by fitting the turnover numbers (TON) as a function of time with the exponential expression $Y = a - bc^x$ for all complexes. The turnover numbers were calculated according to the following equation:

$$\frac{\mathrm{I(GSSG)}}{\mathrm{I(GSH)} + \mathrm{I(GSSG)}} \times \frac{[\mathrm{GSH}]^{\circ}}{[\mathrm{complex}]}$$

where I_{GSSG} and I_{GSH} are the integrals of the resonances relative to the β-CH_2 protons of the cystinyl fragment of GSSG and to the β-CH_2 protons of the cysteinyl fragment of GSH, respectively. The turnover frequencies were obtained as a derivative of the fitting function for *x* corresponding to the incubation time at approximately 50% conversion of GSH to GSSG.

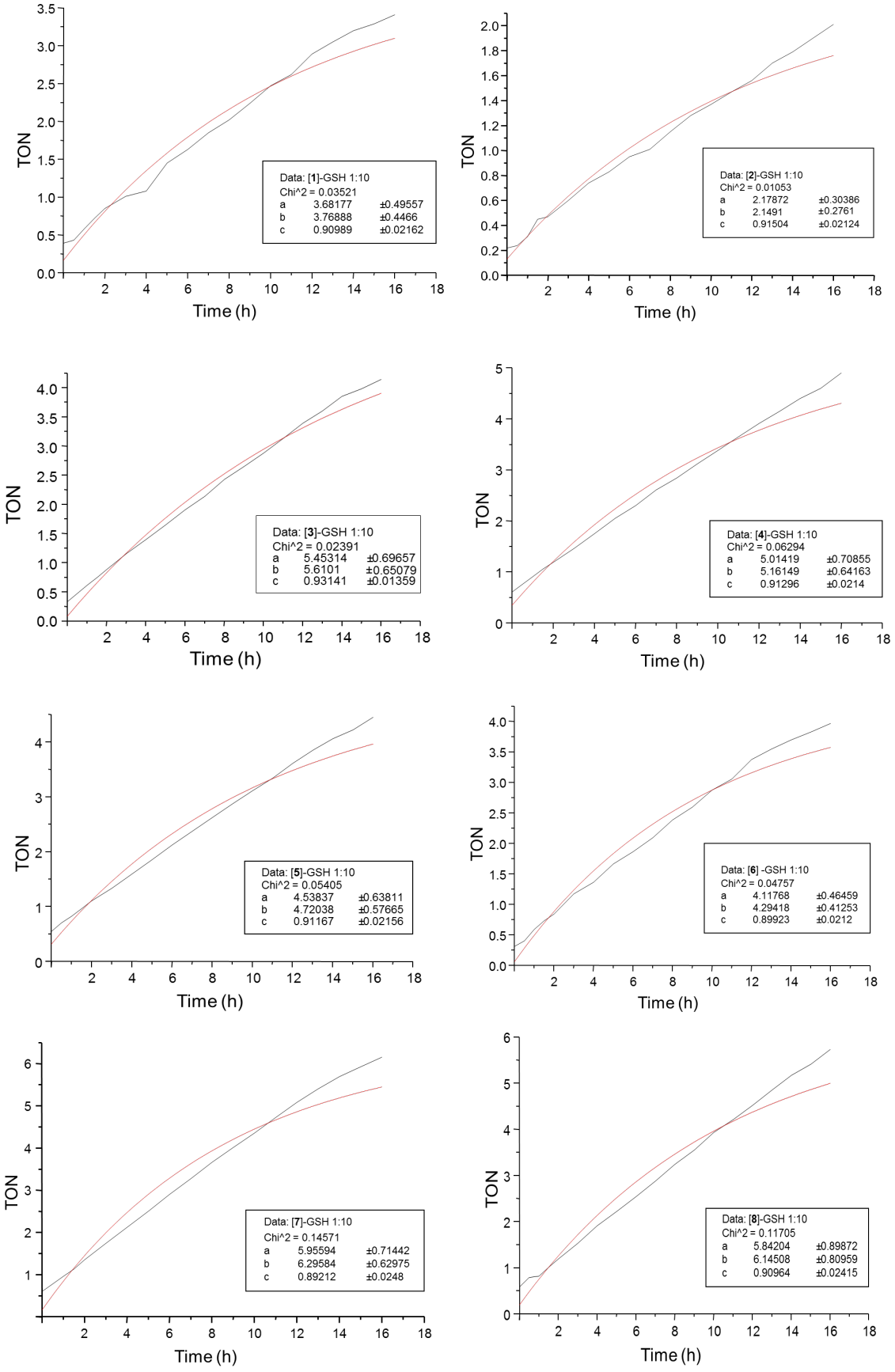

Figure S2. Experimental data (grey curves) and calculated functions (red curve) in the determination of the turnover number for the oxidation of GSH to GSSG for complexes **1**–**8**.

References

1 (*a*) J. W. Wang, K. Moseley and P. M. Maitlis, *J. Am. Chem. Soc*., 1969, **91**, 5970; (*b*) C. White, A. Yates and P. M. Maitlis, *Inorg. Synth*., 1992, **29**, 228.

2 G. M. Sheldrick, *Acta Cryst.*, 2008, **A64,** 112.

3 L. J. Farrugia, *J. Appl. Cryst.*, 1997, **30**, 565.

4 T. Mosmann, *J. Immun. Meth.*, 1983, **65**, 55.